ORIGINAL PAPER

Characteristics of 2009 L'Aquila earthquake with an emphasis on earthquake prediction and geotechnical damage

Ömer AYDAN*¹, Halil KUMSAR*², Selçuk TOPRAK*³ and Giovanni BARLA*⁴

Abstract

The 2009 L'Aquila earthquake with moment magnitude Mw 6.3 occurred in the Abruzzi Region in Central Italy. The earthquake caused the loss of 294 lives and the casualties were particularly heavy in the old city of L'Aquila. The authors have readily investigated the damages due to this earthquake, which was caused by a normal fault with the heavily damaged part being on the hanging-wall side of the causative fault. Approximately 2 weeks before the earthquake, a technician involved with radon monitoring warned that an earthquake will strike the region and this claim was dismissed by the authorities who were heavily questioned by the Italian and International mass media. This article describes the scientific and engineering aspects of the earthquake with emphasis on earthquake prediction and geotechnical damage. Furthermore, the main causes of the heavy structural damage as well as the prediction of the earthquake are discussed. The close inspection of prediction claims indicated that prediction did not really satisfy the requirements for earthquake prediction. The causes of the heavy damage were low seismic resistance of structures and lack of implementation of modern seismic design codes.

1. INTRODUCTION

An intra-plate earthquake with moment magnitude Mw 6.3 occurred in L'Aquila, in Central Italy, at 3:32 local time on April 6, 2009. The earthquake was caused by a normal fault along the Apennines. 294 people were killed in L'Aquila city and nearby villages and towns. The village of Onna was completely destroyed by the earthquake.

Although the magnitude of the earthquake was intermediate, the damage in the old part of L'Aquila city, Onna village and towns of Paganica and Tempara, located on the hanging-wall side of the causative fault, was extremely heavy. The earthquake effects were distinctly observed in a 20 km long and 10km wide area. Some surface ruptures were observed along the expected surface trace of the earthquake fault. Nevertheless, the surface ruptures were not distinct.

Radon anomaly was reported by a technician working at the Gran Sasso National Institute of Nuclear Physics in Assergi about two weeks before the earthquake. Authorities missed the warning and due to this they were strongly questioned by Italian and international media. The short-term regional seismicity was of great interest and may have some implications for observed radon anomaly.

The inferred faulting mechanism of very young faults observed in Paganica town was quite similar to the faulting mechanism of the main shock and previous earthquakes. This deserves great attention in relation to the faulting mechanism of potential earthquakes, which may be of great relevance for earthquake hazard assessment.

This earthquake was quite important in terms of scientific and engineering aspects. The magnitude and structural effects anticipated from paleo-seismological studies and evaluations can be actually validated by this earthquake. The performance and damage of historical architectural structures due to this earthquake also have important implications for assessing the magnitude of historical earthquakes inferred from the damage

reports.

The authors have investigated this earthquake from April 19 to 23, 2009. Although the time was short and there were many restrictions to access to the damaged areas, the authors were able to evaluate the characteristics of the earthquake in terms of earthquake science and earthquake engineering aspects. The evaluations and studies of various reports and regional seismicity of the region before the main shock were of great significance for earthquake prediction and scientific assessment of the claims by a technician involved with radon monitoring. This earthquake also showed the vulnerability and geotechnical damage of natural rock structures during earthquake besides the damage of engineered structures. This article presents the outcomes of the investigations carried out.

2. GEOLOGY AND SEISMO-TECTONICS

The stratigraphy of the earthquake area consists of schists, limestone, lacustrine deposits, conglomeratic deposits and Holocene deposits from bottom to top. Schists are best seen at the east portal of Gran-Sasso tunnel. Schists are overlain by limestone, which is the main rock unit forming Gran-Sasso Mountain ridge (Figure 1). The basin of L'Aquila consists of lacustrine clayey deposits (Figure 2) covered by a conglomerate with inclusions originating from limestone and other rocks from nearby mountains. Matrix of conglomeratic deposits is clayey or calcareous, which can be easily dissolved by ground water flow. All these deposits are covered by Holocene deposits in the Aterno River Valley, formed as a mixture of clay, silt, sand and gravel.

The Italian peninsula is an anti-clock wise rotating platelet squeezed between the Euro-Asia and Africa plates. The Adriatic platelet, which subducts beneath the Italian peninsula and Eurasia plate, is also anti-clock wise rotating (Figure 3). Nevertheless, the northeast motion of the African plate governs the main driving sources of the motions of these platelets. These motions resulted in the formation of the Tyrrhenian back arc basin inducing a plate thinning. As a result, the thinning action together with the anti-clock wise rotation of the Italian Peninsula causes earthquakes with the current normal faulting regime in the Appenines Mountain
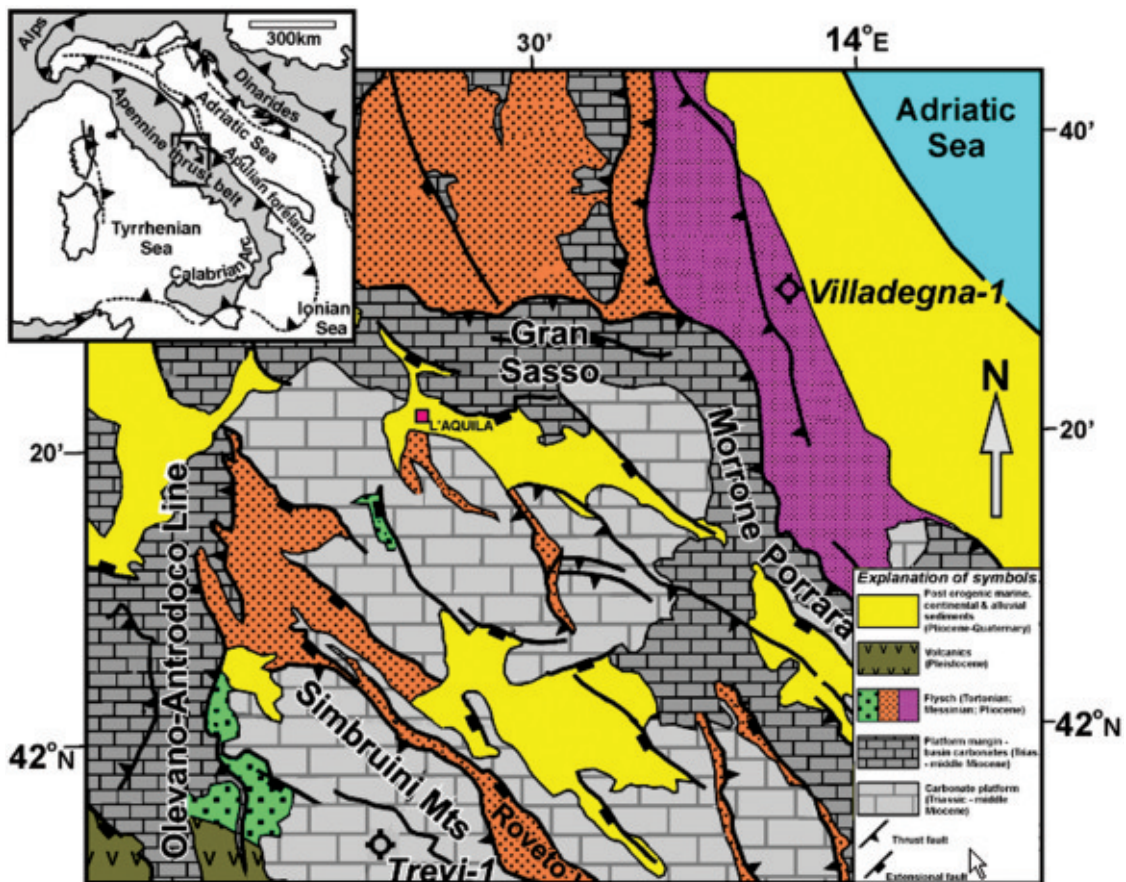

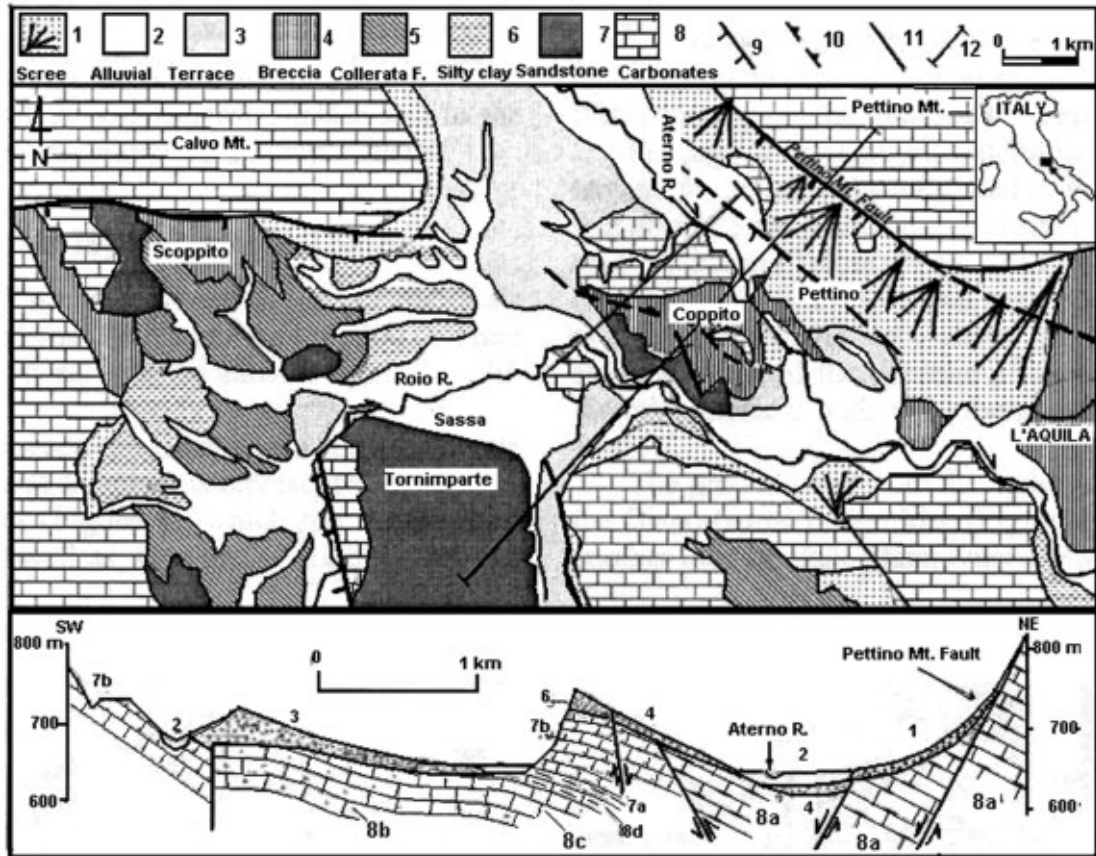**Figure 1.** Regional geological map (modified from Bigi *et al*. 1990).

Figure 2. Geology of L'Aquila and its close vicinity（from Petitta and Tallini, 2003）.

Figure 3. Plate tectonics map（slightly modified from Devoti *et al*., 2008）.

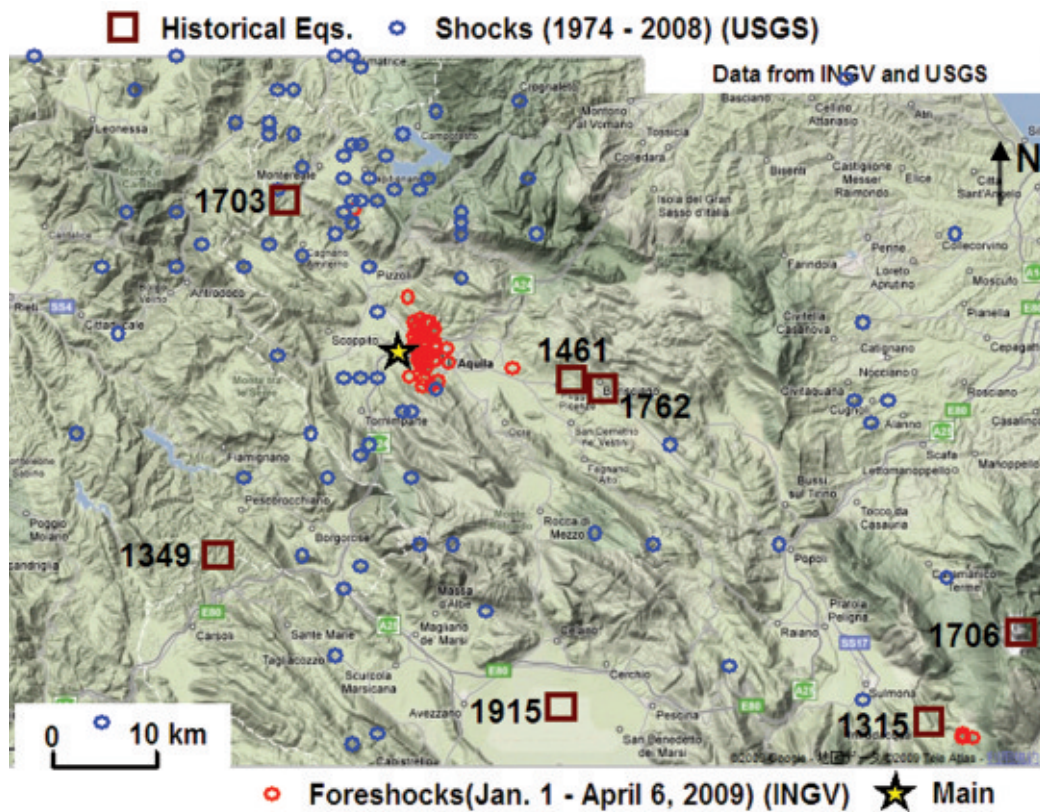Ömer AYDAN, Halil KUMSAR, Selcuk TOPRAK and Giovanni BARLA

Figure 4. Major past earthquakes and regional seismicity before the earthquake.

Range and volcanic eruptions in the vicinity of Sicily Island.

Large historical earthquakes have occurred in the area in 1315, 1349, 1461, 1703, 1706, and 1915. The 1915 event named as Fucino earthquake and had surface magnitude Ms 7 (Figure 4). The most recent events are 1984 Greco (local magnitude Ml 5.8) and 1996 Umbria (Ms 6.1) earthquakes. The nearest event in the vicinity of L'Aquila was the 1461 event. Bagh *et al*. (2007) studied the faulting mechanism of earthquakes in the close vicinity of L'Aquila and found that these were either due to purely normal faulting or oblique faulting with a normal component. They pointed out that there was no large seismic event since the 1915 Fucino event, implying that the region may suffer a large event in near future. This estimation was fulfilled by the 2009 L"Aquila earthquake, although its anticipated maximum magnitude was about 7.

3. CHARACTERISTICS OF THE EARTHQUAKE

3.1 Faulting and Surface Ruptures

The fundamental parameters of the 2009 L'Aquila earthquake have been determined by various seismological institutes worldwide and the results are summarized in Table 1. The estimations indicated that the earthquake was caused by a normal fault 15–20 km long and 10–15 km wide (Figure 5), and the estimated rupture duration ranged between 6.8 and 14 s. In the same table also given are the parameters estimated from empirical relations proposed by Aydan (2007) and measured by the reconnaissance team (Ö.A.) the active fault cutting through the most recent sedimentary deposits (probably of Holocene age) at Paganica is shown in Figure 6. It is particularly interesting to note that the parameters of the active fault observed at Paganica are nearly the same as those of focal plane solutions estimated by several seismological institutes.

Surface ruptures were observed during the reconnaissance mission at Paganica, Lake Sinizzo, Onna and Fossa Bridge (Figure 7). Surface ruptures were observed at three locations in Paganica town. Most of the fractures at Paganica indicated the opening of surface cracks with a normal displacement.

Cracks were also observed on the road to Lake Sinizzo, which is thought to be the southeast end of the earthquake fault. There were also surface cracks in the vicinity of damaged or collapsed bridges on the Aterno River near Onna and Fossa towns. Some of the cracks were of compressive type while most of them were of

Table 1. Fundamental parameters of earthquake estimated by different institutes

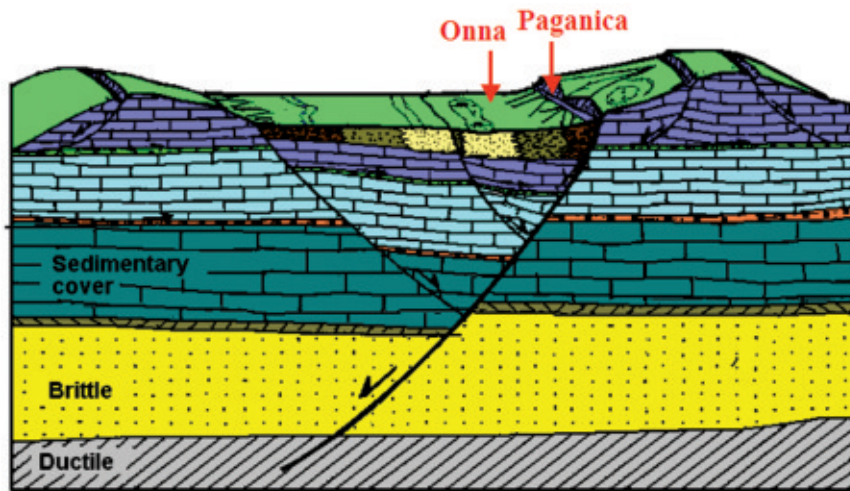| Institute	Mw	Strike	Dip	Rake	Rlip (cm)	Duration (s)	Length (km)	Width (km)
USGS	6.3	127	50	−109		6.8		
HARVARD	6.3	147	43	−88		6.0		
CEA	6.4	139	43	−93		8.4	20	
INGV	6.3	147	43	−88	40		18	16
ERI	6.2	147	44	−99	50	14	25	15
NU	6.3	145	41	−94	60	10	20	10
Ö.A.	6.3	140	52	88	45	8.3	17.5	13.5

Figure 5. Schematic illustration of size and surface effects of M6 class graben earthquakes (modified from Dramis and Blumetti, 2005).
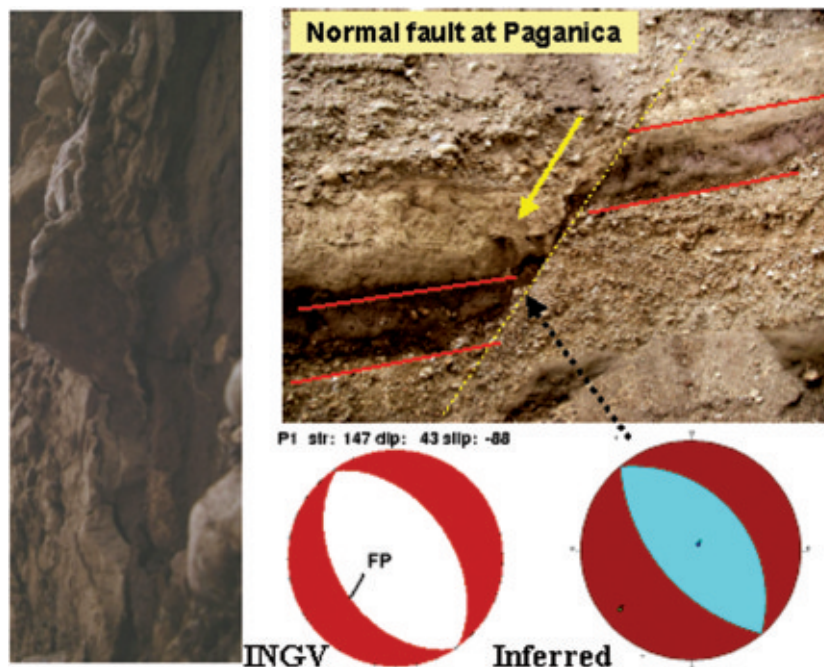

Figure 6. A very young fault in Paganica and comparison of inferred focal mechanism.

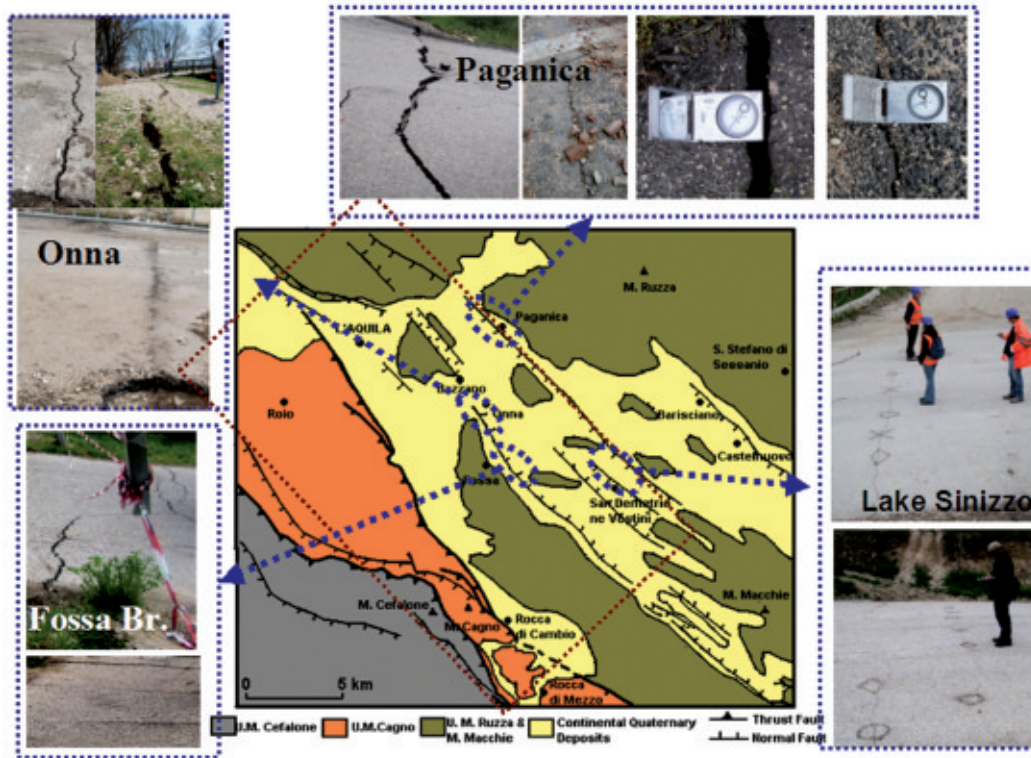Ömer AYDAN, Halil KUMSAR, Selcuk TOPRAK and Giovanni BARLA

Figure 7. Locations and pictures of surface ruptures.

extension type. As the inferred permanent ground displacement from InSAR technique (INGV, 2009) concentrates along the Aterno River, the surface ruptures seen in these localities may also imply that the extension of L'Aquila basin in NE-SW direction, which is a graben structure and the Aterno River flows at the lowest elevation of the basin. The geological group of INGV (2009) also reported that surface fractures occurred at Paganica extending to the north of the A24 Motorway, which may imply that some surface ruptures might pass beneath the viaducts of this motorway. In addition, surface ruptures near Bazzano as well as north of L'Aquila were also reported.

3.2 Shocks and Faulting mechanism

The area is seismically active and it is really difficult to define the time for foreshock activity. Nevertheless, the seismic activity (M>3) was relatively low until 2008 (Figure 4). It started to increase from March 10 and reached a peak on March 30, 2009 (Figure 8). The activity continued during April and there was a foreshock magnitude 4.0 at a distance of 10km northeast of the main shock. The technician (G. Giuliani) from Gran Sasso National Institute of Nuclear Physics, involved with radon monitoring, alarmed by this seismic activity and radon activity, has reportedly warned the people

town of Sulmona about 30 km south-east of L'Aquila and claimed that an earthquake would have occurred on March 29, 2009.

There is no report on the radon monitoring results or on the scientific reasoning to make such a prediction. The earthquake occurred on April 6, 2009 and 30 km away from the anticipated location. Although there were two foreshocks in the vicinity of Sulmona (see Figure 2 for location), most of foreshocks were concentrated in the vicinity of the main shock. The anomaly of radon emission could be undoubtedly associated with the earthquake. This simple example showed that the use of a single parameter could not be decisive. He could have used the foreshock activity in addition to the monitoring of radon emissions. Therefore, none of the fundamental requirements for the prediction of earthquakes (i.e. location, time, and magnitude) was fulfilled by Dr. Giuliani's prediction.

The main shock with moment magnitude Mw 6.3 (Ml=5.8) occurred at 03:33 am local time on April 6, 2009 near L'Aquila. INGV (2009) estimated that the earthquake was as a result of normal faulting on a NW-SE oriented structure about 15 km long. The fault dips toward southwest and the town of L'Aquila is on the hanging wall of the fault just above it. This fault may be associated with the Paganica fault (INGV, 2009).
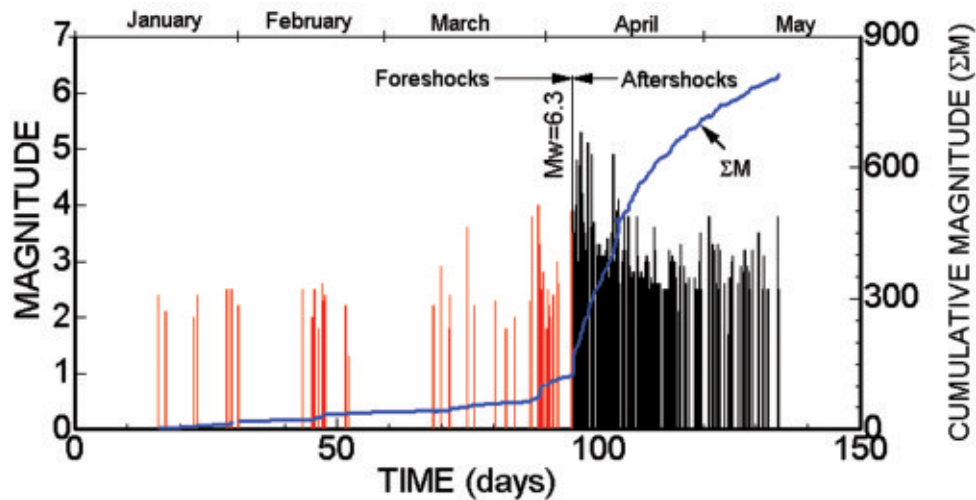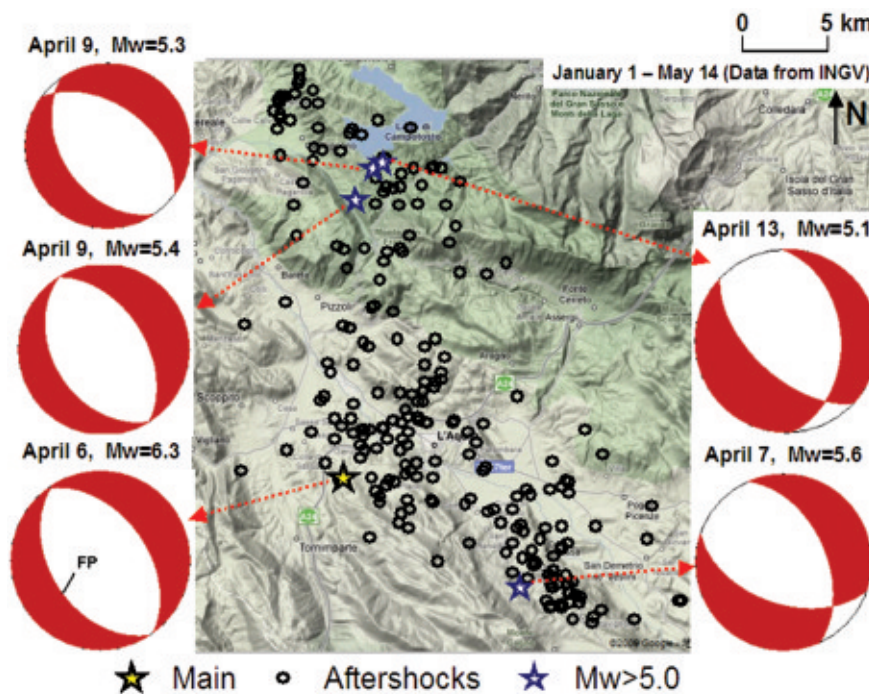
Figure 8. Time history of shocks.

Figure 9. Epicenters of shocks and focal mechanism of some large aftershocks.

Following the main shock, several hundreds aftershocks were recorded (Figures 8 and 9). Three large aftershocks with local magnitude Ml of 4.8, 4.7 and 5.3, respectively occurred on April 7 near L'Aquila and southeast of the city (close to Onna, Fossa and Ocre villages). None of the aftershocks on April 8 was larger than Ml 4. On April 9th, an aftershock with a magnitude Ml 5.1 occurred to the north of L'Aquila, close to Barete, Pizzoli and Campotosto. This is probably the activation of another shorter segment called Campotosto fault of the normal fault system of the Abruzzi Region and the extension of the accumulated seismic stress release towards northwest.

The projection of the aftershock activity on a cross-section perpendicular (NE-SW direction) to the Paganica fault implies that the L'Aquila graben was activated. The focal mechanisms of aftershocks determined by INGV (2009) implied dominantly normal faulting. However, the dip of some of these aftershocks is expected to be northeast in addition to aftershocks with southwest dipping faulting.

3.3 Strong Motion Records

Based on the Italian National Strong Motion Net-

Ömer AYDAN, Halil KUMSAR, Selcuk TOPRAK and Giovanni BARLA

work (Accelerometric National Network (RAN)), 56 strong motion records triggered during the earthquake were so far released (Figure 10). In the close vicinity of L'Aquila, there are four strong motion stations as shown in Table 2: AQV (GX066-B), AQG (FA030-B), AQA (CU104-B) and AQK (AM043-C). They are all on the hanging wall side of the earthquake fault. The equivalent shear wave velocity in the 30 m from the ground surface V_{s30} is in the range 455–1000 m/s. The maximum ground acceleration (6.46 m/s²) was recorded at AQV.

Figure 11 shows the acceleration records at the AQV and AQK stations. It is of great interest that the ground motions are not symmetric with respect to time axis and their form is different from each other, although the epicentral distances and equivalent ground shear wave velocity (V_{s30}) are almost the same. The details of ground conditions of the stations are not available yet; however, the estimates of ground motion amplification based on V_{s30} approach may not be valid at all.

Figure 12 shows the acceleration records at the GSA and GSG strong motion stations, which are reportedly founded on Eocene limestone with a shear wave velocity of 1 km/s. The GSA station is at Assergi and the GSG station is located in an underground gallery. Although the epicentral distances and ground conditions are the same, the acceleration at ground surface is amplified almost 15 times that in the underground gallery.

Figure 13 shows the attenuation of maximum ground acceleration for two different models. Figure 13 (a) is a comparison of attenuation of maximum ground acceleration as a function of hypocentral distance using various attenuation relations. As seen from this figure, attenuation based on spherical symmetry could not estimate a wide range of observational data. The attenuation relation proposed Aydan and Ohta (2006) (see also Aydan 2007) with consideration of fault orientation (θ) and ground characteristics (V_s) provide
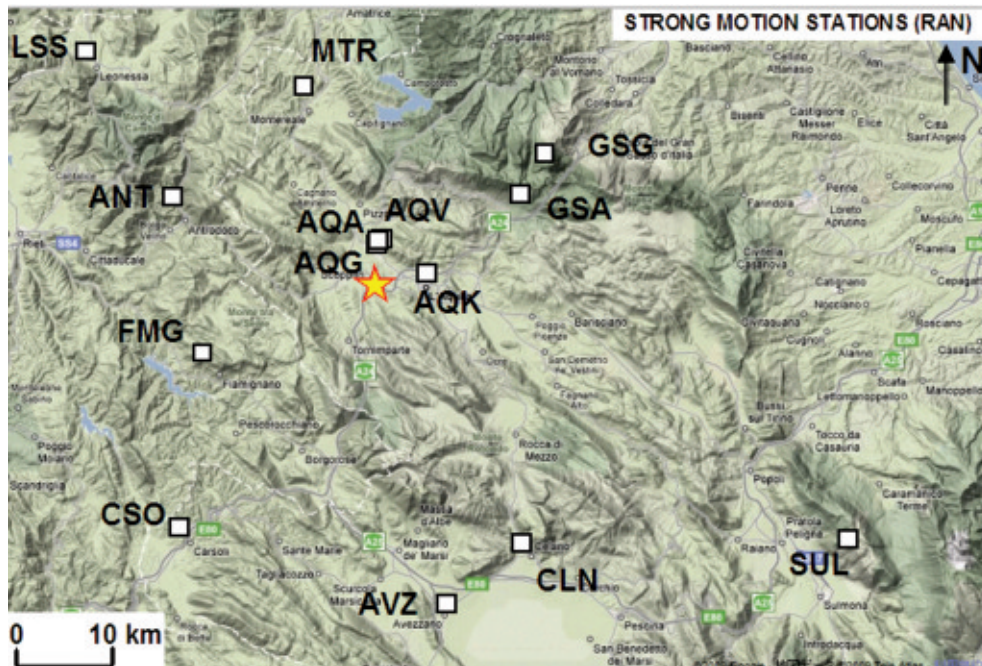

Figure 10. Locations of strong motion stations in the vicinity of the epicenter.

Table 2. Strong motion stations in the vicinity of L'Aquila

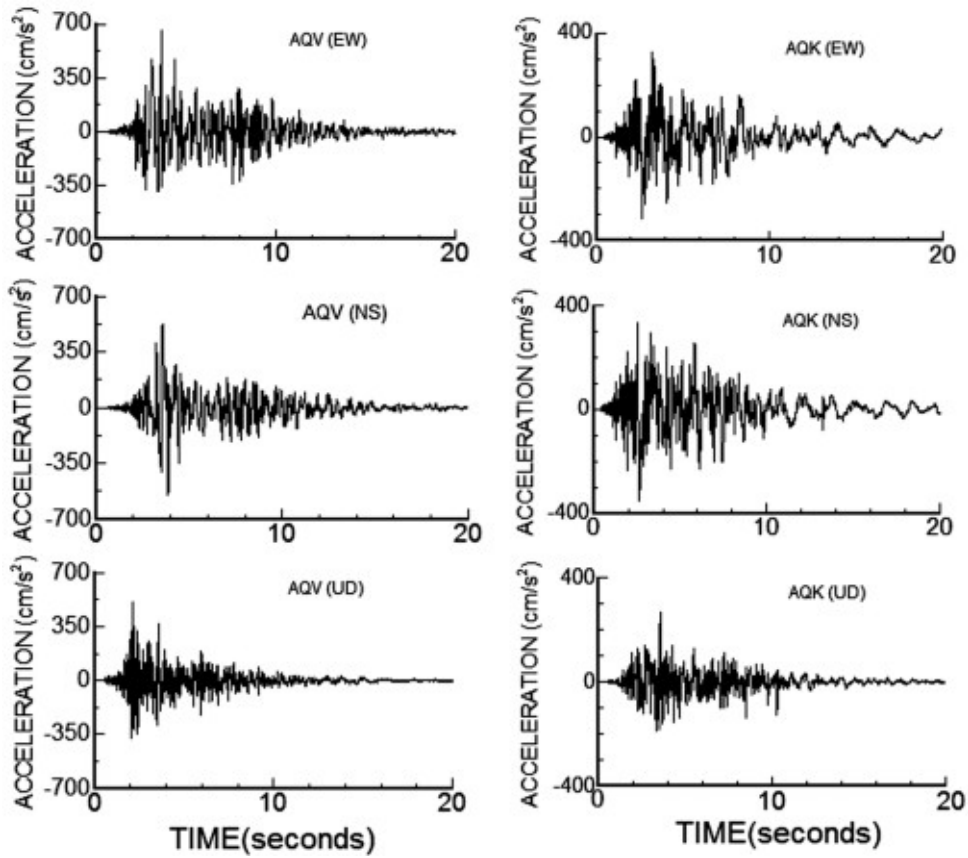| Station name	Station code	Latitude	Longitude	Type of ground	R_e (km)	V_{s30} (m/s)	A_{max} (m/s²)
Aquil Park	AQK	42.345	13.401	Conglomerate	5.6	455	3.66
V. F.Aterno	AQV	42.377	13.337	Fluvial	5.8	475	6.46
Colle Grilli	AQG	42.376	13.339	Limestone	4.3	1000	5.05
V.&F. Aterno	AQA	42.345	13.401	Fluvial	4.8	475	4.78

Figure 11. Acceleration records at AQV and AQK strong motion stations.
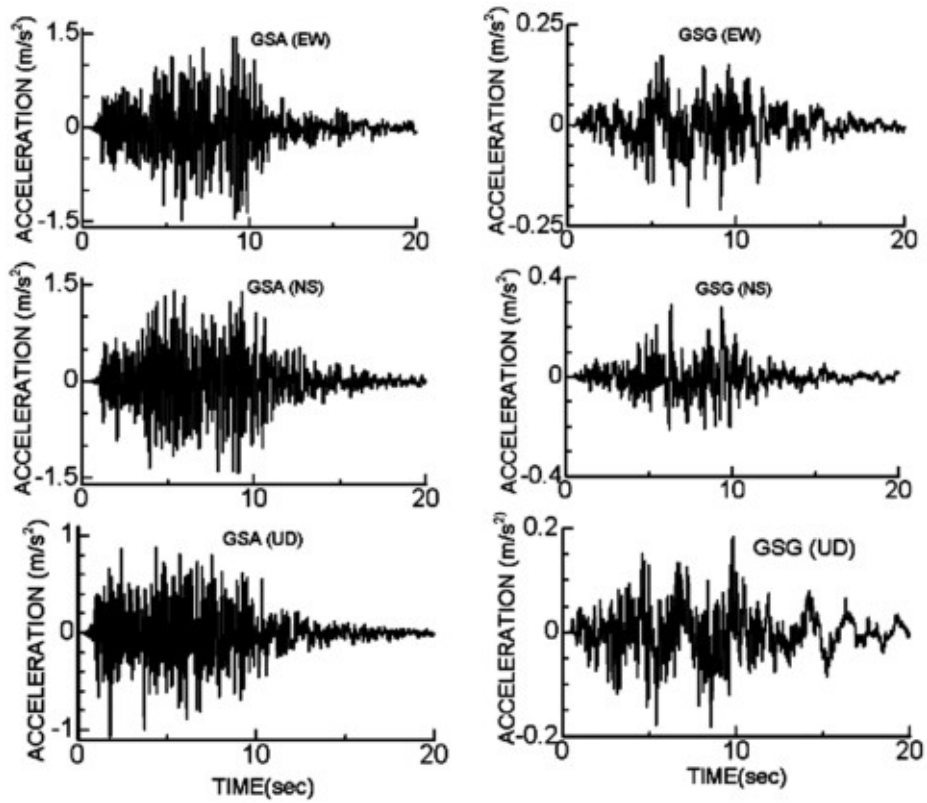
Figure 12. Acceleration records at GSA and GSG strong motion stations.

Ömer AYDAN, Halil KUMSAR, Selcuk TOPRAK and Giovanni BARLA

(a) Spherical attenuation relations   (b) Estimation by Aydan & Ohta relation
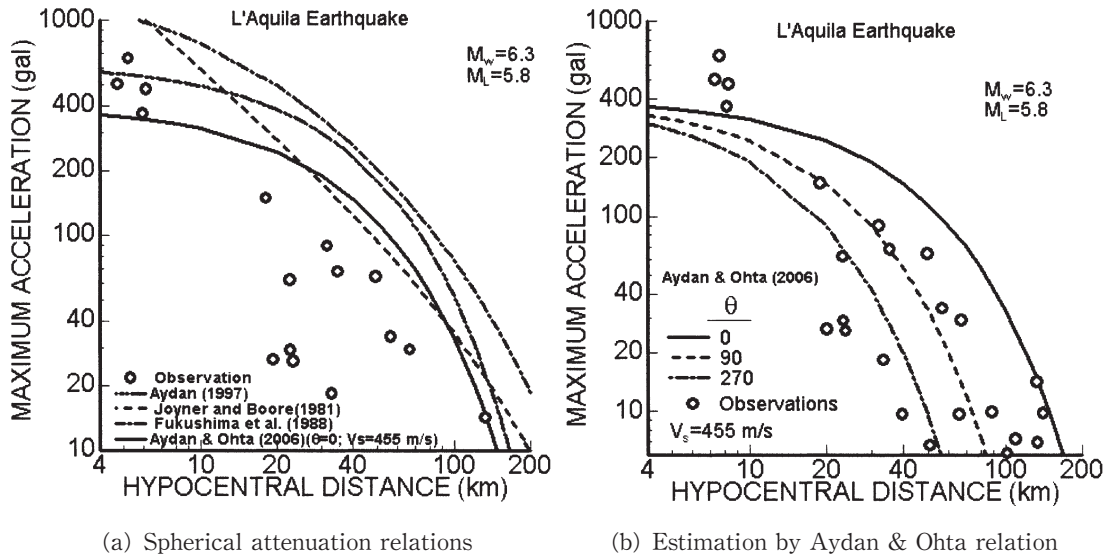
Figure 13. Comparison of attenuation relations with observational data.
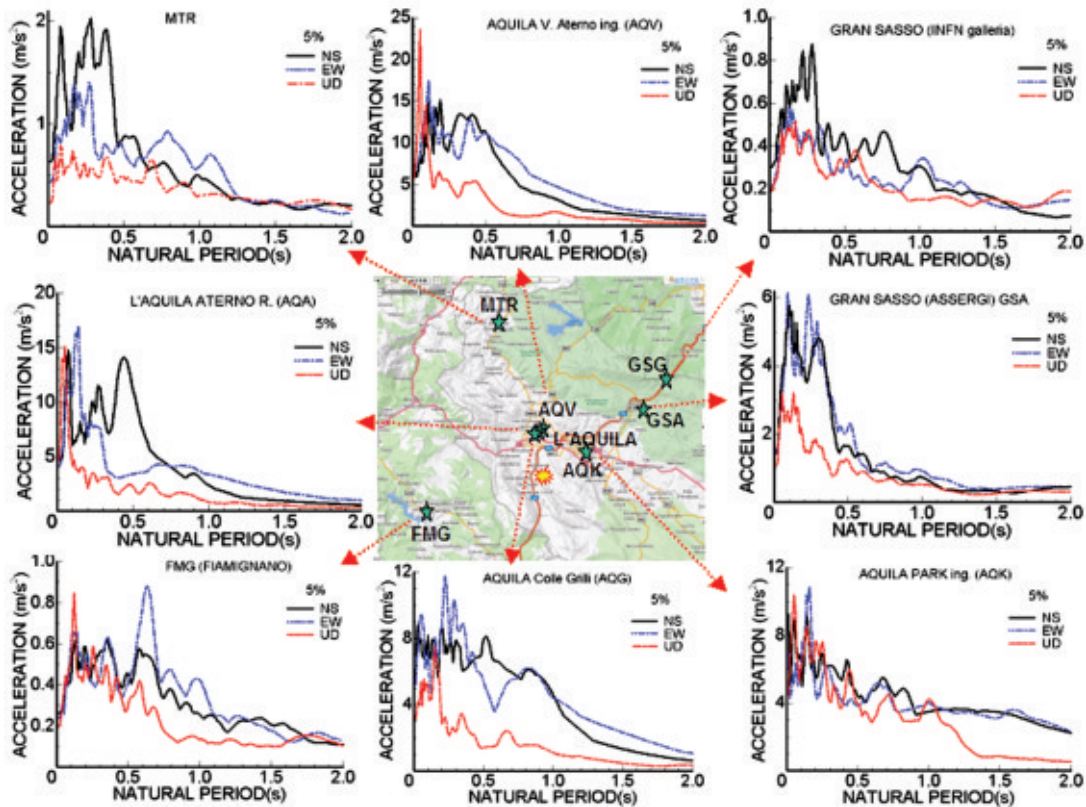

Figure 14. Acceleration response spectra of selected strong motion stations.

better bounds for the observational data.

Figure 14 shows the acceleration spectra of selected stations in the vicinity of the epicenter. When the response spectra of records of strong motion stations in the close vicinity of L'Aquila are compared with the design spectra designated by Eurocode 8 – EC8, the actual response spectra exceed the designations within the period range of 0-0.4s. The base ground acceleration

is expected to range between 0.3 and 0.4g in the downtown of L'Aquila, in view of the ground motion records at the AQK strong motion station and the level of the damage to structures.

Acceleration spectra of some selected strong motion stations (AQV, AQK, AQA, AQG, MTR, FMG, GSA, GSG) are shown in Figure 6. As expected, the spectral accelerations of vertical component are high

for natural periods ranging between 0.05s and 0.1s. As for horizontal component, the natural periods ranges between 0.05s and 0.4s. Nevertheless, very long period components are particularly noted for AQG station, which is located over the bedrock of limestone and it was pointed out by Luca *et al*. (2005), previously.

3.4 Permanent Ground Deformations

An attempt was made to estimate the permanent ground deformations from strong motion records using the EPS method proposed by Ohta and Aydan (2007a, 2007b). The most important aspect of this method is how to assign parameters for numerical integration.

The record is divided into three segments. Filtering is imposed in the first and third segments while the integration is directly applied to the second segment if the acceleration record does not drift. The duration of the second segment is directly based on the rupture process of the earthquake fault.

In view of the rupture process estimated by several institutes and the relation proposed by Aydan (2007), the rupture time was selected as 10s and the filtering of acceleration levels for the first and third segments were and gals. The computed results for station AQA and GSG, which are perpendicular to the fault strike are shown in Figure 15. Figure 16 shows the horizontal
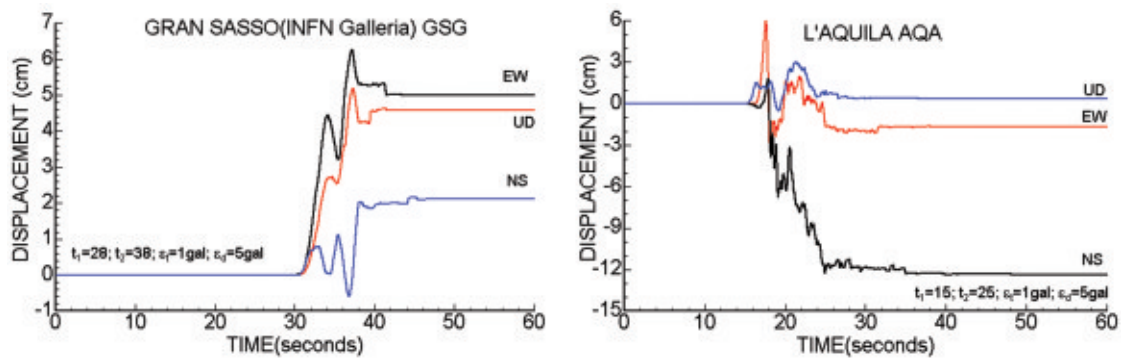

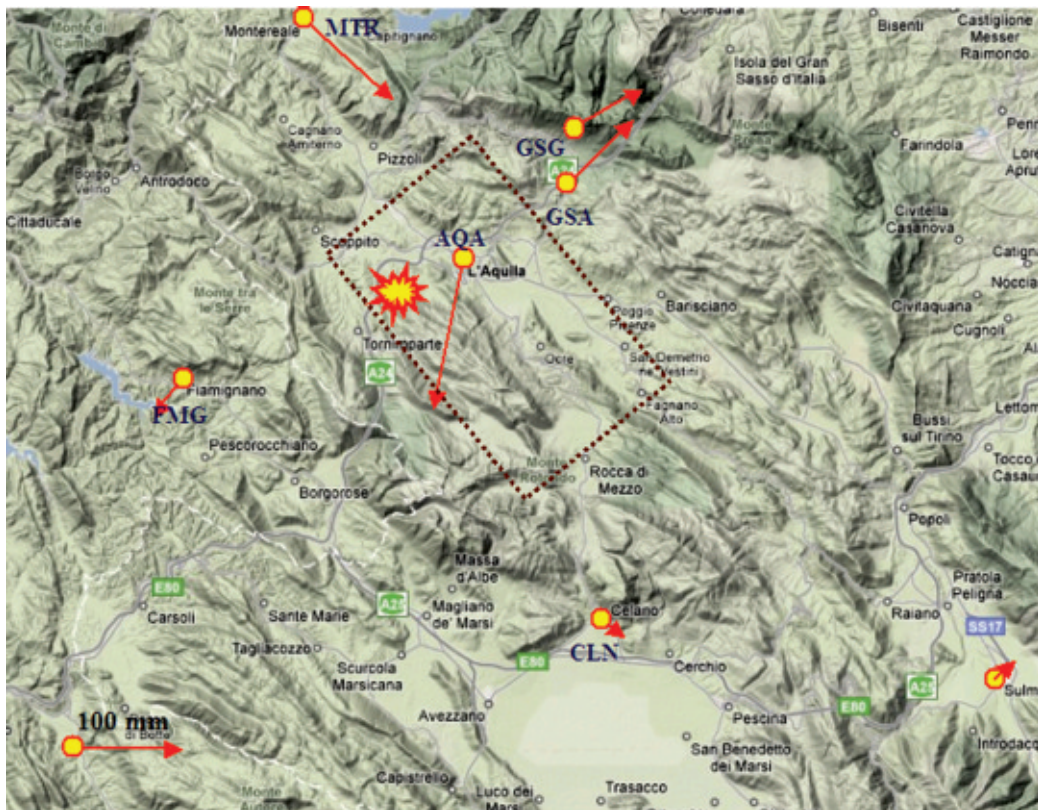**Figure 15.** Estimated ground movements during earthquake at selected points.

Figure 16. Estimated permanent ground displacements by EPS method.

permanent ground deformations, which are comparable with GPS measurements.

4. GEOTECHNICAL DAMAGE

Based on visual inspections, detailed observations, and mapping work performed at different sites during the reconnaissance mission, a number of geotechnical damages and problems are reported in the following. The cases described are not only those occurred; they are rather those observed directly.

4.1 Horizontal movements and cracks

Horizontal movements and cracks were observed in the area of the Aterno River to the west of Onna. The embankments on both sides of the Aterno River moved towards the river creating separation cracks as well as some compression cracks in the vicinity of a damaged bridge as shown in Figure 17. The cracks in the east side of the river were more intensive as the ground was inclined towards west. Nevertheless, no sand boiling was observed.

Based on InSAR evaluation, ground movements are large in the close vicinity of Aterno River near Onna. Tectonic movements, ground liquefaction or both might have caused these movements. If ground liquefaction is involved, it is likely that there is a thick impermeable silty and clayey layer on top of the liquefiable ground below.

4.2 Ground failure at Sinizzo lake

The Abruzzi region is karstic and many sinkholes and dolines exist in the epicentral area. The Sinizzo lake is a doline lake with embankment reinforcement on its northwest side (Figure 18). The lake is 9.8m deep and it has an average diameter of 122.7m (Bertini *et al*. 1989). Extensive ground failures took place around the shore (Figure 19). Although the surrounding ground is mainly calcareous conglomerate, the lake bed is composed of Holocene deposits.

The mechanical properties of ground are not known for this site, yet. However, some preliminary analyses were carried out to evaluate the likely conditions involved with the ground failures, which were observed
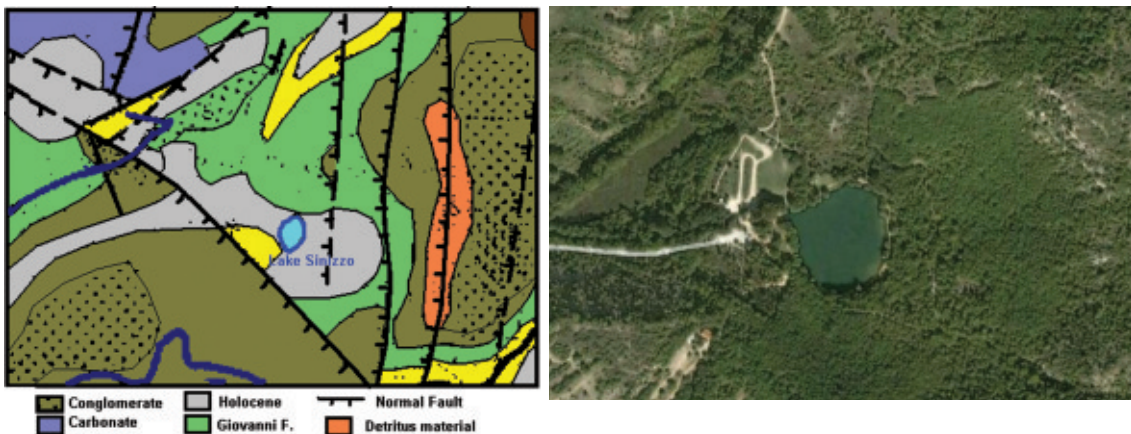

Figure 17. Views of cracking.

Figure 18. Geology and satellite image of Sinizzo lake and its close vicinity.
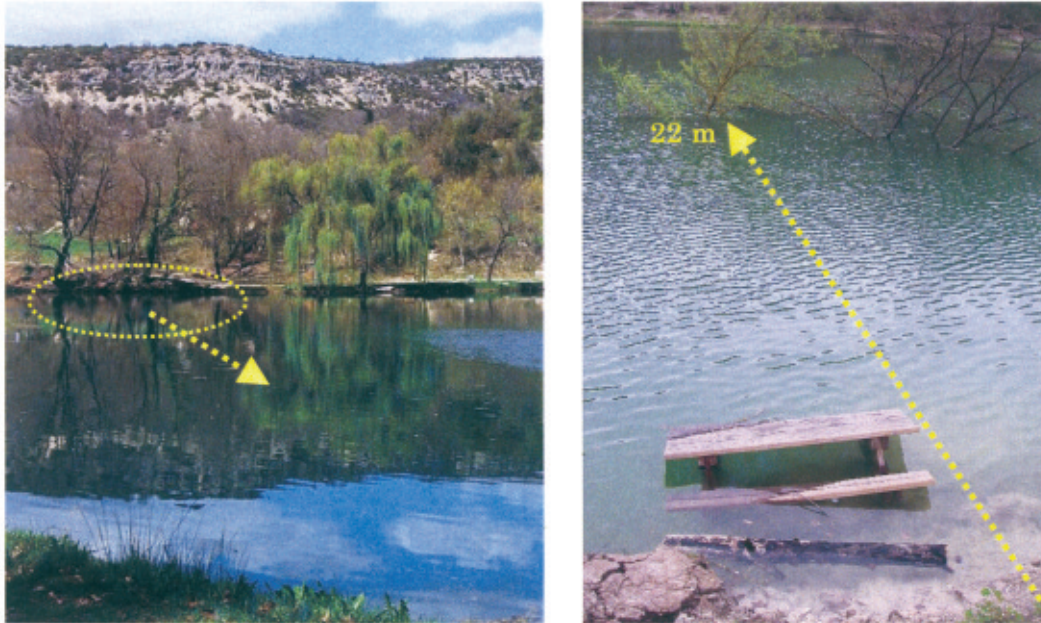
Figure 19.　Views of ground failure before and after the earthquake.

in detail. A series of trial and error computations were carried to obtain material properties, which yield the displacement values close to the measured values. The computational results are shown in Figures 20 and 21 by using the strong motion records of the AQG station. The estimated maximum ground acceleration from a toppled rock block on the north side of the lake was about 0.38g, which is very close to that measured at the station.

Figure 20 shows the movement of the failed ground mass in space, while Figure 21 depicts the time-history of displacement response of the mass center, Shear strength properties of the sliding surface, unit weight of ground and saturation condition are also given in Figure 21. Although further experimental studies are needed to obtain the physical and mechanical properties of the sliding surface, the estimations seem to be quite reasonable in view of properties of similar ground.

4.3 Slope failures and rockfalls

Slope failures caused by the 2009 L'Aquila earthquake may be classified into three categories: a) Soil slope failures; b) Surficial slides of weathered rock slopes c) Rock slope failures （Planar sliding, Wedge sliding failure, and Flexural or Block toppling）, and d) Rock falls. As the magnitude of the earthquake was small and the duration of shaking was short, the scale of slope failures was small. Nevertheless, rock falls induced damage to structures and roadways. Soil slope failures were also observed along the Aterno river shores, and in mountainous areas such as in the vicinity of Campotosto. Figure 22（a）shows a soil slope failure along the Aterno River in Martini District and Figure 22（b）illustrates a soil slope failure near Paganica.

Weathered rock slope failures are of surficial sliding type and rock generally consists of weathered marl, limestone and conglomerate. Figure 23 shows some examples of failure of weathered rock slopes. Particularly marl is very prone to weathering due to cyclic wetting and drying. Furthermore, as the elevation of the epicentral region is very high, the effect of freezing and thawing should be another cause of heavy weathering of rocks.
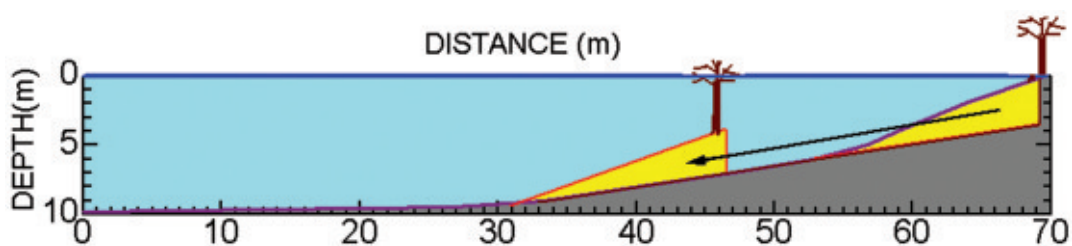

Figure 20.　Lakebed profile and inferred movement of the failed body of ground.
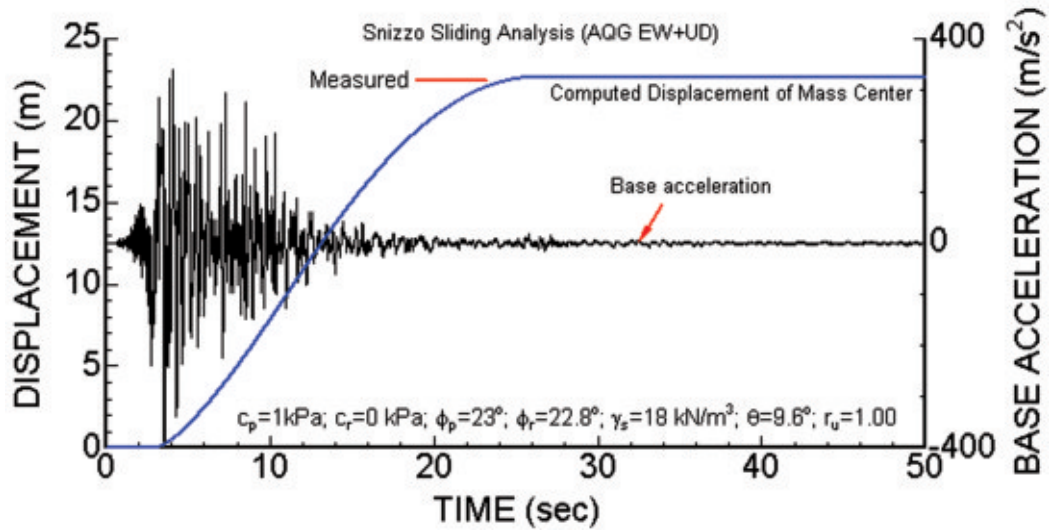
Figure 21. Time history of displacement of mass center of the failed body of ground.

(a) Martini district   (b) Paganica quarry

Figure 22. Examples of soil slope failures.

Failures of rock slopes were observed in the vicinity of lake Sinizzo (Figure 23(a)), of a quarry near Bazanno and Fossa, and roadway cut slopes (Figure 23(b)). Most of rock slope failures involve natural discontinuities such as faults, joints and bedding planes. Depending on the orientation of rock discontinuities, the slope failures may be classified as planar and/or wedge sliding failures, toppling or combined sliding and toppling failures.

Aydan (Aydan, 2007; Aydan *et al*., 2009) has recently proposed some empirical formulas to assess the bounds for slope failures in relation to their natural state and the relative position of the slope with respect to the hypocenter and earthquake fault, and with the considerations of the hanging-wall and footwall effects. These empirical relations are applied to the observations made in this earthquake together with some previ-

(a) Sinizzo   (b) Quarry near Bazanno

Figure 23. Examples of rock slope failures.

ous case histories as shown in Figure 24. It is noted that the observations made during L'Aquila earthquake are generally in accordance with empirical bounds and other previous case history data.

Rock falls were observed in the areas where steep rock slopes and cliffs outcrop. Large scale rock falls were observed in the vicinity of Stiffe, San Demetrio ne' Vestini and lake Sinizzo and Paganica (Figure 25). Some of these rock falls induced damage to structures. It is well known that rock falls occur following failure initiation of individual rock blocks in sliding, toppling or combined sliding and toppling modes. Therefore, it is of interest to back analyse the initation of the rock fall observed in the vicinity of Stiffe due to sliding motion. The size of fallen block of limestone was approximately 190x150x160 cm³. The rock fall is initiated when relative sliding exceeds its half width. As the thickness of the block is about 160 cm, the possible half width range of the block should vary between 75 and 95 cm. The base

inclination of the block is taken as 20° in view of the limestone bedding inclination in the vicinity of Stiffe. Figure 26 shows the computational results for the record taken at the AQG station under half saturated conditions, as there is no acceleration record in the vicinity of Stiffe. The static and kinetic friction angles of the interface between the base and block was taken as 35° and 30° in view of experimental results available to the authors for the bedding planes of Alpine limestone. Although it is essential to perform rock mechanics tests on the interface characteristics of the fallen rock block, the chosen values should be sufficient for this preliminary analysis. For the chosen values of interface properties, the computed relative displacement is 94.7 cm. If the shortest side of the block is selected, the block would definitely start to fall. If the other side is chosen, it would be at a limiting state. As the measured size of the block is approximate, the computed results should be sufficient to explain why the rock block fall occurred. A
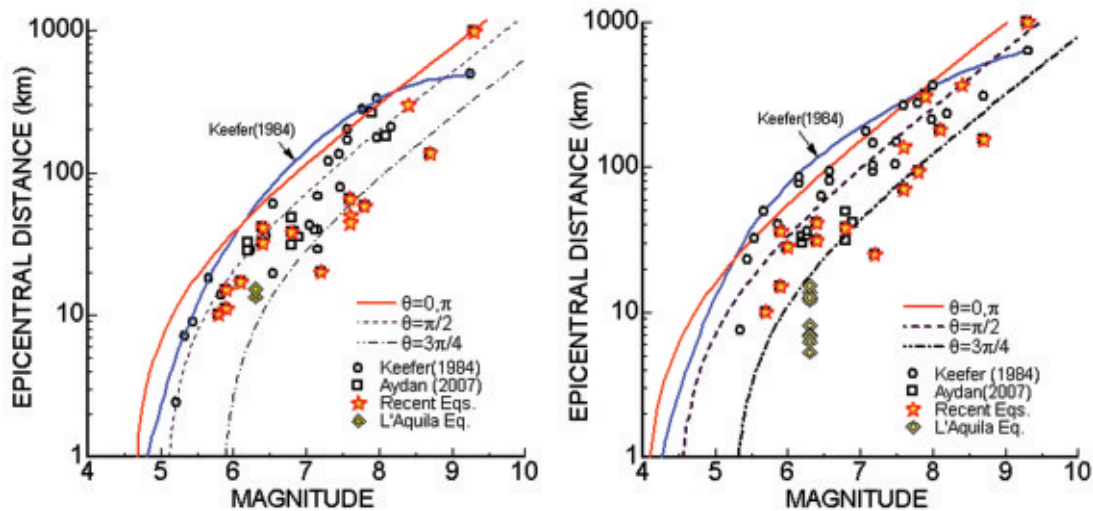

Figure 24. Comparison of data of L'Aquila earthquake with empirical bounds.

(a) San Demetro ne' Vesti   (b) Stiffe

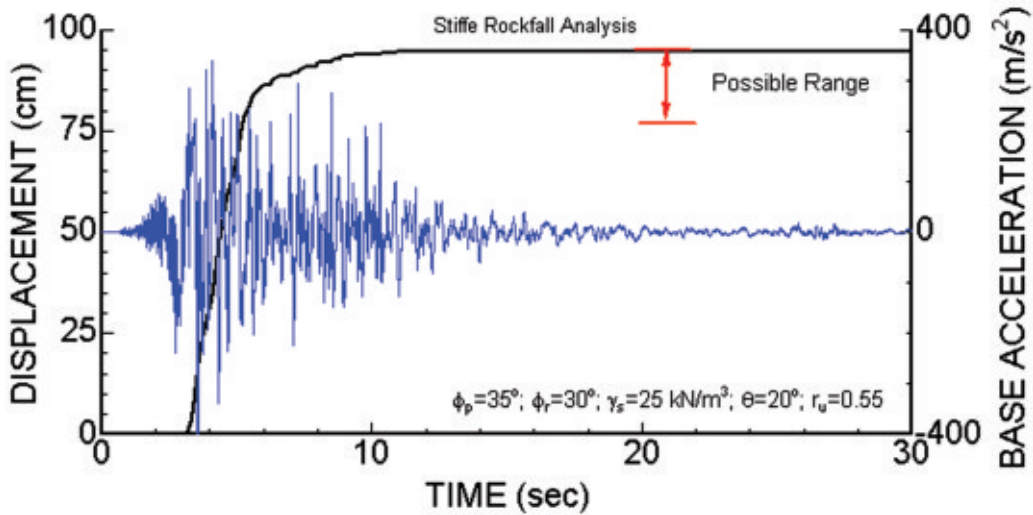**Figure 25.** Examples of rock falls.

Figure 26. Computational results for the initiation of rock fall at Stiffe.

toppling mode failure was not possible as the applied acceleration was less than 0.43 g.

As shown in Figure 25(a), overhanging slopes of conglomeratic deposits were fallen at San Demetrio ne' Vestini. The surfaces of the fallen blocks imply that they have failed in tension. The dynamic stability of these fallen overhanging slopes may be analysed by considering a flexural toppling mode (Aydan and Kawamoto 1987, 1992). The overhanging length of the fallen blocks due to flexural toppling failure was about 150 to 170 cm, while their thickness about 100 cm. Figure 27 shows the computational results for a tensile strength ranging between 180 and 200 kPa while the unit weight

of rock was assumed to be 20 kN/m³. Furthermore, the ratio of vertical to horizontal acceleration was assumed to be 0.85, with the consideration of measured maximum acceleration values. The matrix of conglomerate is calcareous and it is relatively weak. The estimation of the tensile strength of conglomerate at this site seems to be quite acceptable. In the same site, there are many overhanging conglomerate layers. The length of stable overhanging conglomerate layers observed is generally less than 100–120 cm. These observations are in accordance with the computational results.

Finally, with reference to rock slope failures, it is of interest to analyse some of the observed cases in the
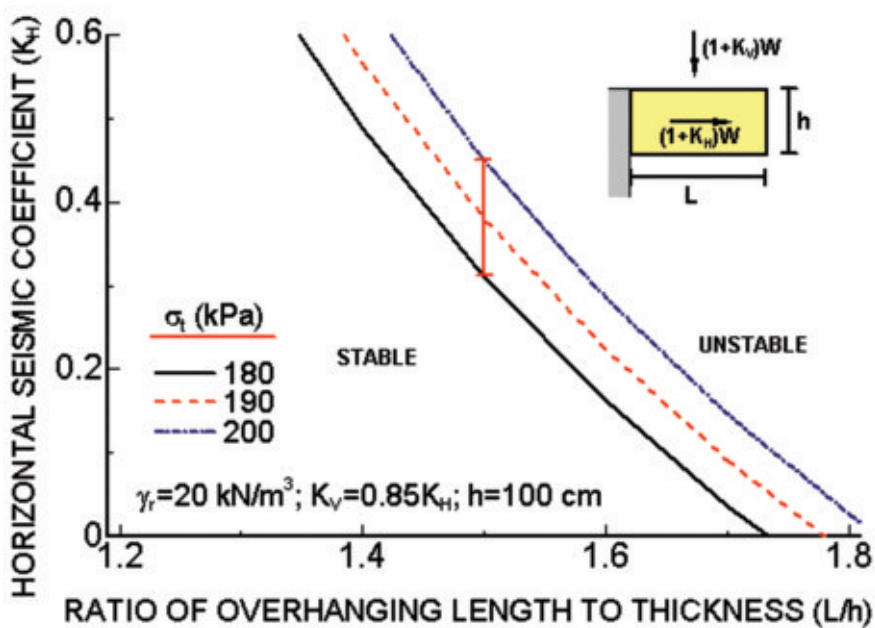

Figure 27. Computational results for failed overhanging slopes at San Demetrio.

light of the methods of Aydan and his colleagues (Aydan *et al.*, 1989; Aydan and Kawamoto, 1992; Kumsar *et al.* 2000; Aydan and Kumsar, 2009). Figure 28 compares results with observational data from stable and unstable slopes. The data compiled by the first author from natural rock slopes of Apennines are also plotted.

Apennines are composed of limestone and other calcareous rocks of different geologic age. As a result, their stability is influenced by the orientation of the bedding planes as well as normal faults. During the compilation of data, it was noted that, when layers are thin, the slope angle for stability under natural conditions is drastically reduced. Furthermore, when layers dip into the slope, the naturally stable slope angle tends to be almost equal to that of the bedding plane. For layers dipping into the mountainside, the stable slope angle is almost equal to or greater than that of the normal to the bedding planes. When it is greater than the angle of normal, its value ranges from 5° to 35°. When the slope becomes higher, the stable slope angle tends to converge to that of the normal to the bedding plane. The angle of repose of a slope debris ranges between 30° and 40°. Figure 28 was prepared as a guideline for local engineers to select the slope-cutting angles to be adopted in actual restoration of the failed slopes.

4.4 Sinkholes and caves

The geology of L'Aquila involves limestone at the base, lacustrine clay and continental debris in the form of conglomerate and breccias and Holocene alluvial deposits from bottom to top. The L'Aquila breccia of Pleistocene age is known to contain karstic caves. Karstic caves are geologically well known and generally form along steep fault zones and fractures due to erosion as well as solution by ground water (i.e. Aydan and Tokashiki, 2007).

During the reconnaissance mission, the authors paid attention to two large karstic caves, which are both very close to the AQK strong motion station (Figure 29). Their height is about 5 m. Along the same road one can easily notice the remnant of karstic caves on a rock-slope cut. It seems that karstic caves are a well-known problem in L'Aquila; one may find a number of reports regarding the search of potential karstic caves using various geophysical methods (i.e. Tallini *et al.*, 2004a,b).

The L'Aquila earthquake caused a number of sinkholes in L'Aquila (Figure 29 and Table 3). One of the sinkholes was well publicized worldwide. The width was about 10 m and its depth is not well-known. A car was fallen into it. Another sinkhole had a slightly smaller size. Its length and width were about 8 m and 7 m, respectively. The depth was about 10 m. The layers between the roof and road level were breccia with calcareous cementation, breccia with clayey matrix and top soil from bottom to top. A side trench was excavated to a depth of 3 to 4 m from the ground surface on the
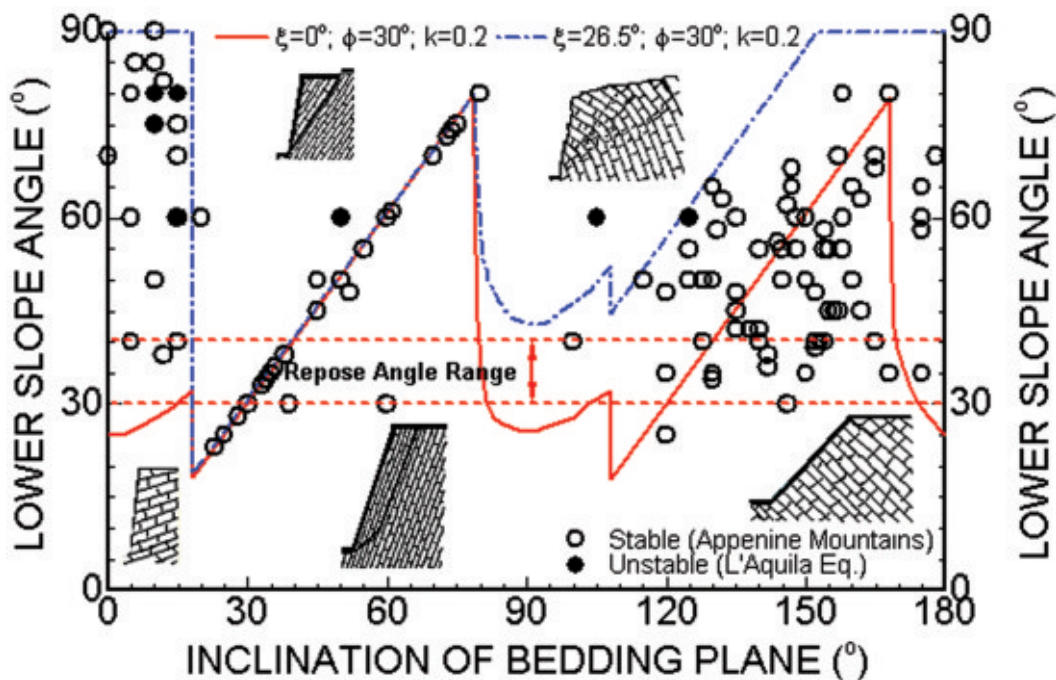

Figure 28. Comparison of observational data with computational results prom previous studies
(ξ: intermittency angle; k: horizontal seismic coefficient; φ: friction angle).

Figure 29. Sinkholes in L'Aquila.

Table 3. Major parameters of sinkholes（please note that the values are approximate）

L1 (m)	L2 (m)	h (m)	h* (m)	Amax-EW (a/g)	Amax-NS (a/g)	Amax-UD (a/g)	Location
6	10	3	3	0.341	0.383	0.365	L'Aquila-S1
7	6	3	3	0.341	0.383	0.365	L'Aquila-S1
3	5	1.5	1	–	–	–	Castel-Nuovo

south side of the sinkhole. The reconnaissance team of the GEER from USA also reported that a sinkhole occurred in Castelnuovo and it had a length and width of 5 and 3 m respectively, with a depth of 5 m. The roof thickness was about 1.5–2.5 m.

Figure 30 illustrates the results obtained with a mathematical model, which has been developed in order to back analyse the instabilities of the sinkholes obser-

ved. Observational values of EW and NS horizontal component of ground accelerations taken at AQK strong motion station were used.

The ratio of vertical seismic coefficient to horizontal seismic coefficient was taken as 0.85 in view of measurement results. The roof thickness was assumed to be 300 cm, while the surcharge load height was varied between 0 cm and 300 cm. The unit weight and tensile
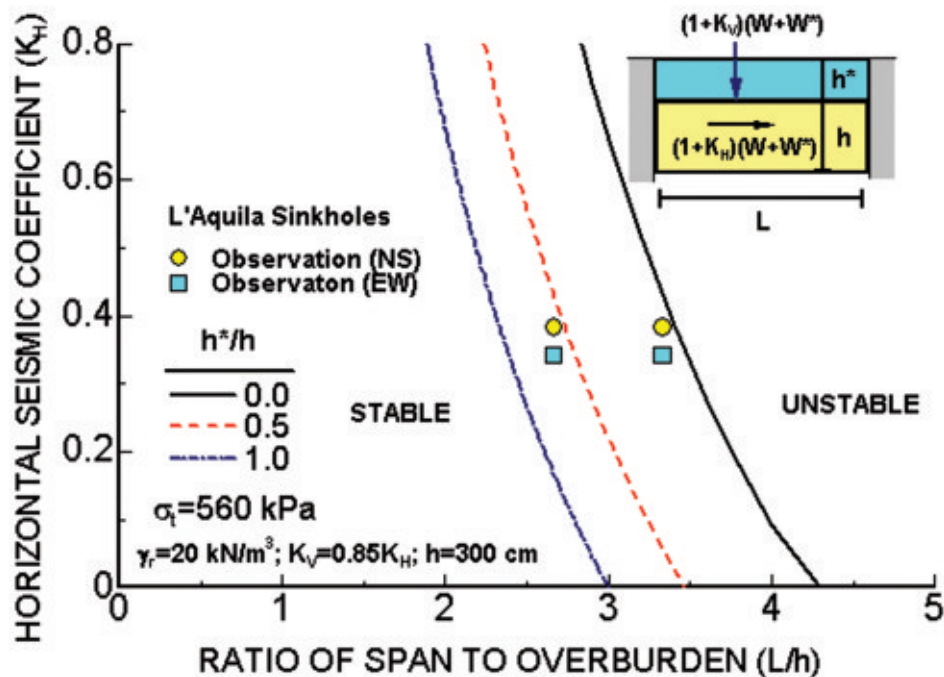

Figure 30. Comparison of computational results with observational results.

strength of the roof material were assumed to be 20 kN/m³ and 560 kPa, respectively. The site observations indicated that a 300 cm deep trench was excavated on one side of the sinkhole site. Therefore, the trench excavations for sewage pipes drastically reduced the effective roof thickness. As expected, the increase of surcharge load drastically reduces the seismic resistance of roof of karstic caves.

The ratio of the longest dimension of sinkholes to roof thickness is plotted in the same Figure 30 using the maximum EW and NS horizontal acceleration values. The case histories fall in the unstable domain computed with the mathematical model using the material properties and measured geometries of sinkholes. The tensile strength of the in-situ rock mass is remarkably similar to the observations made on Ryukyu limestone caves and cliffs in Japan (Tokashiki and Aydan, 2008). From these computational and observational results it may be concluded that the deep sewage trench excavation and high ground acceleration played a major role in causing the instability of karstic caves resulting in sinkholes in

L'Aquila. As the 1703 event caused similar sinkholes, it is clear that the sinkhole phenomenon repeats itself at each earthquake of significant magnitude.

4.5 Ground liquefaction and lateral spreading

Soil liquefaction is caused by generation of pore water pressure and it is often observed when ground consists of fully saturated sandy soil. Alluvium deposits are present along the Aterno River in the epicentral area. During investigations, the authors found sand boils along the Aterno River in the area called Martini, which is just south of the hill on which the old downtown of L'Aquila is located. The river meanders in the area and it is likely to have resulted in sandy deposits at those meanders.

At Martini district liquefaction created many NE-SW trending fractures,parallel to the river embankment as shown in Figure 31. Sand boiling as thick as 150 mm was observed in various locations. The movement of ground was towards SE direction. Table 4 and Figure 32 show some physical properties and grain size distribu-

Figure 31. Ground liquefaction and lateral spreading induced damage and ground settlement at the depot yard in Martini district.

Table 4. Properties of liquefied soil samples collected from sand volcanoes

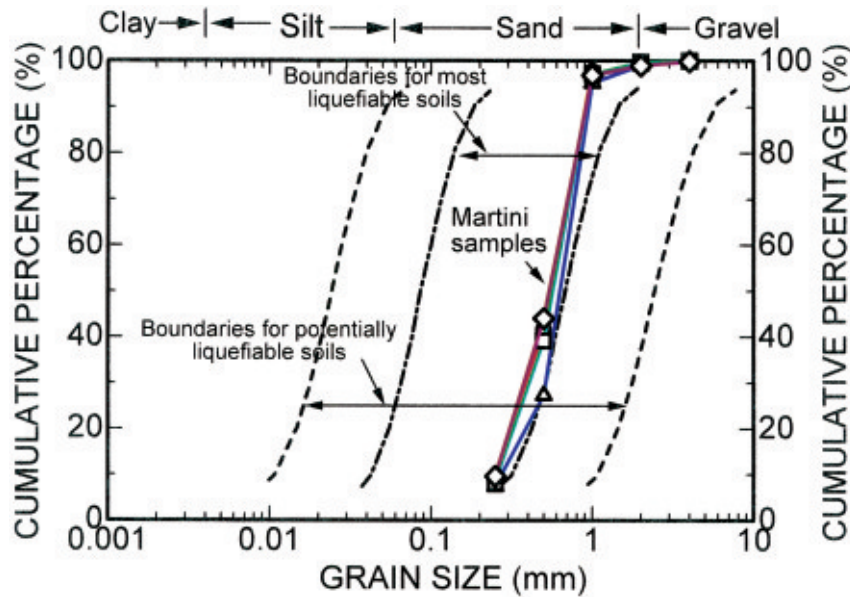| Dry unit weight (kN/m³)	Porosity (%)	Mean grain size D_{50} (mm)	Friction angle (degree)
13.11–13.80	39.0–41.6	0.5–0.6	32–35

Figure 32. Grain size distribution and comparison of liquefaction bounds.

tion of sand boils, respectively. Boiled sand is almost homogenous and its grain size distribution falls within the easily-liquefiable bounds according to Japan Port and Harbour Research Institute classification (1997).

The liquefaction induced lateral spreading. The sum of crack openings from the adjacent field towards the river embankment ranged between 250 and 350 mm. There were several depot-like structures and bridges for railways and roadways in the area where soil liquefaction was observed. However there was no visible damage on the structures, probably because the foundations were resting on deep stiff soil.

Figure 33(a) compares the empirical bounds proposed by several researchers for the limit of ground liquefaction with observations. The observations are within the limits of liquefiable ground. Since the number of data is at present quite limited, new data may give more accurate results.

An attempt was made to obtain the ground deformation due to liquefaction induced lateral spreading using several methods. Aydan *et al*. (2008) proposed a new method based on the maximum ground velocity obtained from the strong motion records. Figure 33(b) compares the estimation of ground deformation for

different layer thickness. The comparison with the observational data implies that the thickness of liquefied ground at Martini district should be ranging between 1.5 and 2 m.

Additional comparative evaluations are based on the use of ground motion data in close vicinity of the liquefaction site of Martini district. Figure 34 compares the estimations with the observation. In the computation, the NS and UD ground motion records of AQK station were used. The residual friction angle ranged between 10 and 14 degrees while keeping the peak friction angle 35 degrees. The observation is close to the computation for 14 degrees residual friction. These evaluations are preliminary and further experimental and computational studies are needed.

5. STRUCTURAL DAMAGE

The same note of caution as that written in introducing the description of geotechnical damages is needed in reporting the structural damage below. The phenomenona observed in this case were so widespread and of a complexity that the considerations in the following are indeed general and limited to visual observations
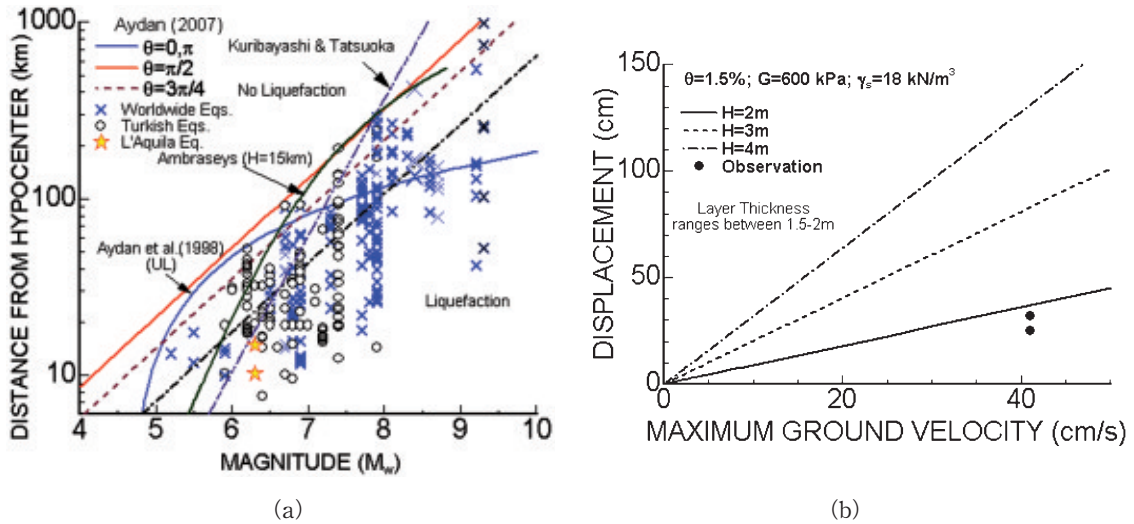
(a)   (b)

Figure 33. Comparison of observations with estimations from the method proposed by Aydan *et al*. (2008) based on maximum ground velocity.
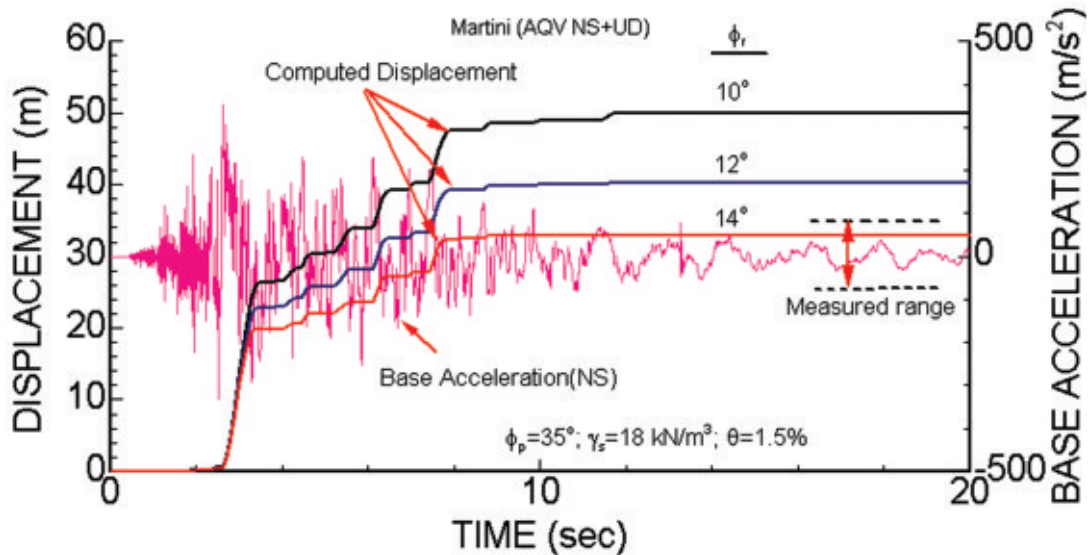

Figure 34. Comparison of observations with estimations from the method proposed by Aydan *et al*. (2008) based on rigid body model.

during the reconnaissance mission.

5.1 Damages to buildings

Masonry buildings can be grouped into residential buildings and cultural and historical buildings. (Figure 35). Residential masonry buildings are generally two story buildings made of stone, brick or mixture of stone and bricks. The mortar is mud or lime. Heavily damaged or collapsed buildings had almost no tie beams. Furthermore, the mortar of these buildings was mud. The main cause for the collapse or heavy damage of masonry buildings was out-of plane failure.

Cultural and historical buildings are of larger scale and involve, domes, towers and facades. The failure mechanism of these buildings is fundamentally quite similar to that of ordinary masonry buildings. The non-existence of tie beams makes these buildings quite vulnerable to heavy damage and collapse. The dome of Santa Maria del Suffragio collapsed although wooden tie beams were used. As the wooden tie beams were not continuous over the perimetry of the dome, its effect was disastrous. The masonry cylindrical tower at Santo Stefano di Sessanio, which is about 20km from the epicenter, was completely collapsed (Figure 36). It is

Figure 35. Examples of masonry building damage.

(a) before   (b) after

Figure 36. Views of the tower of Santo Stefano di Sessanio before and after the earthquake.

important to notice that another tower with almost the same height, located at the foot of the same hill, survived the earthquake. This may be related to the difference in the amplification characteristics of the top and foot of the hill as well as the shape and shaking characteristics of the towers.

Many reinforced concrete (RC) buildings were

either collapsed and heavily damaged by the earthquake (Figure 37). The reasons of the heavy damage or collapse have similarity with those seen in Turkey and elsewhere. The possible reasons are poor workmanship, design and construction mistakes, resonance, lack of moral, weak (soft) floor effects and collision. It was even interesting to note in some of the heavily damaged buildings that

Figure 37. Examples of heavily damaged or collapsed reinforced concrete buildings.

the unwashed sea sand was used for concrete mixture, although L'Aquila is 90 km away from the sea.

5.2 Damage to transportation facilities

A 35 m long and 5 m wide three-span continuous reinforced concrete bridge collapsed as illustrated in Figure 38. It was located at the crossing of the SR261 road on the Aterno River leading to Fossa town. Four reinforced concrete columns with hexagonal section broke at the column-slab connection and slid sideway and penetrated the deck slab. The column had six 17 mm diameter smooth bars at each corner of the hexagonal section. 9 mm diameter smooth bars were also used to fix the top of the columns to the reinforced concrete girders. The stir-ups were 6mm in diameter at a spacing of 300 mm. The vertical downward motion might have played an important effect on the failure of this bridge. Also a 20 m long and 4 m wide three span continuous bridge just to the west of Onna suffered damage at the top of the frame piers. The superstructure of the bridge was damaged by tensile cracking due to movement of piers towards the center of the river due to movements of the embankment on the both sides.

A 2 m long and 2.5 m high stone masonry arch bridge collapsed and was repaired by filling crushed limestone into the collapsed section as seen in Figure 38.

Figure 38. Collapse bridges and damaged road surfacing.

The southwest side abutments (Figure 38) were probably moved towards west and this movement resulted in the loss of arching effect, and collapse during the earthquake. Furthermore, the infill cover of this bridge was thin. This may be also an additional cause for the collapse.

A part of the viaducts of A24 expressway near L' Aquila was affected by the earthquake, although there was no collapse of the expressway anywhere (Figure 39). The viaducts are simply supported PC box-girder bridges supported by reinforced concrete piers. They were supported by steel sliders and roller bearings or elastomeric bearings. The viaduct was displaced and there were gaps as large as 200 mm at numerous locations. A number of decks drifted in the longitudinal and transverse directions. Some of these gaps were repaired by asphalt filling.

5.3 Damages of retaining walls

Settlement of surface roads occurred at a number of locations. One of the two lanes of SS17 at the intersection with SR615 was partly restricted for traffic because the road embankment locally subsided by 350 mm and the upper part of the stone masonry retaining wall tilted as shown in Figure 40. The tilted retaining wall was supported by a wooden support system.

5.4 Damages to water pipelines

Damage to pipelines is generally caused by the

Figure 39. Damage to A24 expressway.

Figure 40. Examples of damage to masonry retaining walls.

permanent ground deformation, which may result from faulting, slope failure, liquefaction induced lateral spreading. The authors observed damage to water pipes in Paganica and near Onna. (Figure 41). The damage to water pipelines in Paganica was caused by the combined effect of faulting as well as slope failure. Pipes failed due to by the extensional movement of the surrounding medium. The damage to the pipe near Onna was caused by the movement of the surrounding ground towards the center of the bridge over the Aterno River. The pipes were damaged at both sides of the river. Nevertheless, the movement was much larger on the eastern side of the bridge and the pipe was buckled.

5.5 Damage to industrial facilities

There are many industrial facilities in the earthquake affected area. There was almost no damage to pre-cast industrial facility structures, which are generally vulnerable to earthquakes. The good design and construction of beam-column joints of these structures could be the main reason for no damage and good performance. However, 20 m high and 4 m diameter silos for storing polypropylene pellets in the VIBAC plant suffered severe buckling problems as seen in Figure 42.

Two types of silos were built at different times. The first group of 8 silos was founded on a common pile foundation and supported by a steel frame structure. The other group consisted of 12 silos, set in two rows on a cylindrical skirt resting on 1.2 m thick concrete slabs on pile foundations. The cylindrical skirt is fixed to the pile cap through anchor bolts. The silos were made of 6 mm thick aluminum plates. The silos, which buckled, were totally full with the material during the earthquake, while those with 65% of their full capacity did not collapse. During the earthquake, the buckled silos

pounded with the adjacent warehouse. The damaged bottom skirts of the silo cones exhibited diamond buckling modes.

6. CONCLUSIONS

L'Aquila earthquake provided valuable lessons on how modern and historical buildings, bridges and other structures behaved under a $M_w = 6.3$ intra-plate basin earthquake. Historically l'Aquila and the vicinity were subjected to at least 8 earthquakes since the 14th century. During this earthquake, extensive damage was developed in the old city of L'Aquila and the towns and villages in its vicinity including Onna, Paganica, Fossa and Ocre. The L'Aquila basin is covered by conglomeratic clayey or calcareous deposits underlaid by lacustrine clayey deposits.

The foreshock activity in the epicentral region was of great importance in relation to earthquake prediction. In-spite of the claims, the earthquake prediction based observed radon anomaly did not satisfy the fundamental requirements for earthquake prediction. However this example clearly illustrates the fact that a multi-parameter integrated scheme must be adopted for earthquake prediction.

Settlements and sliding of ground and geotechnical structures occurred at numerous locations in the lowland along the Aterno River, and a number of slope failures and rockfalls sliding occurred in the mountainous regions. Two sinkholes were observed in the old city of L'Aquila.

Old unreinforced masonry buildings were extremely vulnerable to the earthquake. In particular, unreinforced masonry buildings with mud mortar suffered extensive damage. Out-of plane failure of walls was predominant

(a) Paganica   (b) near Onna

Figure 41. Damaged pipes by permanent ground movement.

Ömer AYDAN, Halil KUMSAR, Selcuk TOPRAK and Giovanni BARLA

Figure 42. Views of buckled silos.

in reinforced concrete frame buildings with unreinforced brick masonry wall. The reasons of the heavy damage or collapse have similarity with those seen in Turkey and elsewhere. The possible reasons are poor workmanship, design and construction mistakes, resonance, lack of moral, weak (soft) floor effects and collision.

The failure mechanism of Cultural and historical buildings these buildings is fundamentally quite similar to that of ordinary masonary buildings. The non-existence of tie beams make these buildings quite vulnerable to heavy damage to collapse. The dome of Santa Maria del Suffragio collapsed as non-continuous wooden tie beams were used. The masonary cylindrical tower at Stefano di Sessanio, which is about 20 km from the epicenter, was completely collapsed while another tower with almost same height located at the foot of the same hill survived the earthquake. This may be related to the difference in the amplication characteristics of the top and foot of the hill as well as the shape and shaking characteristics of the towers. The damage to cultural and historical buildinngs and structures by this earth-

quake may be used to re-evaluate the parameters of past seismic events.

Extensive corrosion of steel bars in reinforced concrete structural members was widely observed not only in buildings but also in bridges. Concrete cover was too thin for preventing corrosion.

A three-span continuous short-span bridge collapsed, and several bridges suffered damage. At A24 viaduct in L'Aquila, residual drift of decks and vertical gaps at the expansion joints occurred due to damage of bearings. However damage of bridges and viaducts was generally limited or non-existent.

ACKNOWLEDGEMENTS

information by the other team members, particularly Prof. Dr. K. Kawashima and Prof. Dr. K. Konagai, are greatly appreciated.

REFERENCES

Ambraseys, N.N. (1988): Engineering Seismology. Earthquake Engineering and Structural Dynamics, V.17, 1-105.

APAT (2006): Carta Geologica d'Italia alla scala 1:50.000 - Foglio n. 359 "L'Aquila". S.EL.CA. Firenze.

Aydan, Ö. (1997): "Seismic characteristics of Turkish earthquakes," *Turkish Earthquake Foundation*, TDV/TR 97-007, 41.

Aydan, Ö. (2000): An stress inference method based on structural geological features for the full-stress components in the earth' crust, *Yerbilimleri*, **22**, 223-236.

Aydan, Ö. (2004): Damage to abandoned lignite mines induced by 2003 Miyagi-Hokubu earthquakes and some considerations on its possible causes. J. of School of Marine Science and Technology, Vol. 2, No. 1, 1-17.

Aydan, Ö. (2007): The inference of seismic and strong motion characteristics of earthquakes from faults with a particular emphasis on Turkish earthquakes. The 6th National Earthquake Engineering Conference of Turkey, 563-574.

Aydan, Ö. (2008): Investigation of the seismic damage to the cave of Gunung Sitoli (Tögi-Ndrawa) by the 2005 Great Nias earthquake. Yerbilimleri, No. 29, No. 1, 1-16.

Aydan, Ö., Geniş, M. (2007): Assessment of dynamic stability of an abandoned room and pillar underground lignite mine (in Turkish). Journal of Rock Mechanics, Turkish National Rock Mechanics Group, ISRM, No. 16, 23-44.

Aydan, Ö. and T. Kawamoto (1987): Toppling failure of discontinuous rock slopes and their stabilisation (in Japanese). *Journal of Japan Mining Society*, **103**(1197), 763-770.

Aydan, Ö. and Kawamoto, T. (1992): The stability of slopes and underground openings against flexural toppling and their stabilisation. *Rock Mechanics and Rock Engineering*, Vol. 25, No. 3, pp. 143-165.

Aydan, Ö., Kawamoto, T. (2004): The damage to abandoned lignite mines caused by the 2003 Miyagi-Hokubu earthquake and some considerations on its causes. 3rd Asian Rock Mechanics Symposium, Kyoto, Vol. 1, 525-530.

Aydan, Ö. and H. Kumsar (2009): An experimental and theoretical approach on the modeling of sliding response of rock wedges under dynamic loading. *Rock Mechanics and Rock Engineering*, (DOI: 10.1007/s00603-009-0043-3).

Aydan, Ö. and Ohta, Y. (2006): The characteristics of strong ground motions in the neighbourhood of earthquake faults and their evaluation. Symposium on the Records and Issues of Recent Great Earthquakes in Japan and Overseas. EEC-JSCE, Tokyo, 114-120.

Aydan, Ö. and Tokashiki, N. (2007): Some damage observations in Ryukyu Limestone Caves of Ishigaki and Miyako islands and their possible relations to the 1771 Meiwa Earthquake. Journal of The School of Marine Science and Technology, Vol. 5, No. 1, pp. 23-39.

Aydan, Ö. and Ulusay, R. (2002): Back analysis of a seismically induced highway embankment failure during the 1999 Duzce earthquake. Environmental Geology **42**, 621-631.

Aydan, Ö., Y. Shimizu, Y. Ichikawa (1989): The Effective Failure Modes and Stability of Slopes in Rock Mass with Two Discontinuity Sets. *Rock Mechanics and Rock Engineering*, **22**(3), 163-188.

Aydan, Ö., Ulusay, R., Kumsar, H., Sönmez, H. and Tuncay, E. (1998): "A site investigation of June 27, 1998 Adana-Ceyhan Earthquake", *Turkish Earthquake Foundation*, TDV/DR 006-03, 131p.

Aydan, Ö., Tano, H., Geniş, M. (2007): Assessment of long-term stability of an abandoned room and pillar underground lignite mine (in Turkish). Journal of Rock Mechanics, Turkish National Rock Mechanics Group, ISRM, No. 16, 1-22.

Aydan, Ö., Ulusay R., Atak, V.O. (2008): Evaluation of ground deformations induced by the 1999 Kocaeli earthquake (Turkey) at selected sites on shorelines. Environmental Geology, Springer Verlag, **54**, 165-182.

Aydan, Ö., Ohta, S., Hamada, M. (2009): Geotechnical evaluation of slope and ground failures during the 8 October 2005 Muzaffarabad Earthquake, Pakistan. Journal of Seismology (DOI: 10.1007/s10950-008-9146-7).

Bagh, S., L. Chiaraluce, P. De Gori, M. Moretti, A. Govoni, C. Chiarabba, P. Di Bartolomeo, M. Romanelli (2007): Background seismicity in the Central Apennines of Italy: The Abruzzo region case study. Tectonophysics, **444**, 80-92.

Bertini T., Bosi C., and Galadini F. (1989): La conca di Fossa-S. Demetrio dei Vestini. In: CNR, Centro di Studio per la Geologia Tecnica, ENEA, P.A.S.: "Elementi di tettonica pliocenico-quaternaria ed indizi di sismicita olocenica nell'Appennino laziale-abruzzese". Societa Geologica Italiana, L'Aquila, 26-58.

Bigi, G., Cosentino, D., Parotto, M., Sartori, M., and Scandone, P. (1990): Structural model of Italy and gravity map. CNR - Progetto Finalizzato Geodinamica, Quaderni de "La Ricerca Scientifica" No. 114, 3, 1990.

CEN, Eurocode 8 (1994): Design provisions for earthquake resitance of structures. European ENV 1998. Comite Eurpeen de Normalisation, Brussels.

Devoti R., Riguzzi F., Cuffaro M., and Doglioni C. (2008): New GPS costraints on the kinematics of the Appeninnes subduction. *Earth Planet Sci. Lett.*, doi: 10.1016/j.epsl.2008.06.031.

Dramis, F. and Blumetti, A.M. (2005): Some considerations concerning seismic geomorphology and paleoseismology. Tectonophysics, **408**, 177-191.

ERI (2009): 2009 April 06 Central Italy Earthquake. Strong Motion Seismology Group. http://taro.eri.u-tokyo.ac.jp/saigai/20090406eq/20090406.html.

EMSC (2009): Special page on L'Aquila earthquake. http://www.emsc-csem.org/

Faccenna, C., Florindo, F. Funicello, R. and Lombardi, S. (1993): Tectonic setting and Sinkhole Features: case histories from western Central Italy. Quaternary Proceedings, **3**, 47-56.

Fukushima Y. Tanaka T. Kataoka S. (1988): A new attenuation relationship for peak ground acceleration derived from strong-motion accelerograms, Proc. 9th World Conf. on Earthquake Engineering 2, Tokyo-Kyoto, Japan, 343-348.

INGV (2009): Special page on L'Aquila earthquake. http://www.ingv.it

Italian Strong Motion Network (RAN managed by the Italian Department of Civil Protection, DPC. (http://www.protezionecivile.it/minisite/).

HARVARD: Source process. http://www.globalcmt.org/cgi-bin/globalcmt-cgi-bin/

Kumsar, H., Aydan, Ö. and Ulusay, R. (2000): Dynamic and static stability of rock slopes against wedge failures. Rock Mechanics and Rock Engineering, Vol. 33, No. 1, 31-51.

Kuribayashi, E. and Tatsuoka, F. (1975): "Brief Review of Soil Liquefaction during Earthquakes in Japan", *Soils and Foundations*, **15**, 4, pp.81-92.

Joyner, W.B. and Boore, D.M. (1981): Peak horizontal acceleration and velocity from strong motion records from the 1979 Imperial Valley California Earthquake. Bull. Seis. Soc. Am., **71**(6), 2011-2038.

Luca, de Luca, S. Marcucci, G. Milana, T. Sano (2005): Evidence of Low-Frequency Amplification in the City of L'Aquila, Central Italy, through a Multidisciplinary Approach Including Strong- and Weak-Motion Data, Ambient Noise, and Numerical Modeling. *Bull Seism*

Soc Am., **95**, 1469-1481.

Magaldi, D. and Tallini, M. (2000): A micromorphological index of soil development for the Quaternary geology research. Catena, **41**, 261-276.

Nisio, S., Caramanna and Ciotoli, G. (2007): Sinkholes in Italy: first results on the inventory and analysis. In Natural and Anthropogenic Hazards in Karst Areas: Recognition, Analysis and Mitigation. Geological Society, London, Special Publications, **279**, 23-45.

Ohta, Y., Aydan, Ö. (2007a): Integration of ground displacement from acceleration records. JSCE Earthquake Engineering Symposium, 1046-1051.

Ohta, Y., Aydan, Ö. (2007b): An integration technique for ground displacement from acceleration records and its application to actual earthquake records. Journal of The School of Marine Science and Technology, Vol. 5, No. 2, 1-12.

Petitta, M. and Tallini, M. (2003): Groundwater resources and human impacts in a Quaternary intramontane basin (L'Aquila Plain, Central Italy). Water International, Vol. **28**(1), 57-69.

Port and Harbour Research Institute, Japan (1997): Handbook on Liquefaction Remediation of Reclaimed Land, Balkema, 312p.

Tallini, M., Giamberardino, A., Ranalli, D. and Scozzafava, M. (2004a): GPR survey for investigation in building foundations. Tenth Inter. Conf. on Ground Penetrating Radar; Delft, Netherlands, 395-397.

Tallini, M., Ranalli, D., Scozzafava, M. and Manocorda, G. (2004b): Testing a new low-frequency GPR antenna on karst environments of Central Italy. Tenth Inter. Conf. on Ground Penetrating Radar; Delft, Netherlands, 133-135.

Tokashiki, N. Aydan, Ö. (2008): The stability assessment of natural rock structures in Ryukyu limestone. 5th Asian Rock Mechanics Symposium (ARMS5), Tehran, 1515-1522.

Tetè P., Pesce G.L. & Leonardis B. (1984): Il Lago Sinizzo nei pressi di San Demetrio Ne Vestini (L'Aquila). Natura.

Yamanaka, Y. (2009): Central Italy earthquake. Nagoya University Earthquake research Center. http://www.seis.nagoya-u.ac.jp/sanchu/Seismo_Note/2009/NGY15.html.

Characteristics of 2009 L'Aquila earthquake with an emphasis on earthquake prediction and geotechnical damage

要　　旨

2009年イタリア中部ラクイラ地震の特徴およびその予知と地盤被害について

　2009年4月6日午前3時32分頃（現地時間）にイタリア中部ラクイラ（L'Aquila）において ML＝5.8，MW＝6.3の地震が発生し，多数の犠牲者を出すなど，大きな被害が生じた．この地震による犠牲者は294名（4月12日現在），負傷者は1,000人以上であった．著者らは(社)土木学会，(社)地盤工学会，(社)日本建築学会および日本地震工学会は，4学会協同による合同調査団のメンバーとして2009年4月18日～23日にかけて，ラクイラ及び周辺地域の現地調査を実施した．本論文でこの地震の特徴，施設の被害とその評価について報告した．本論文の主な結論は下記の通りである．

1）今回の地震で見られた前震活動は地震予知の観点から大変興味深いものであった．しかし，前震活動とラドンガスの異状を元に Gran Sasso 核物理実験所の技術者が地震予知をしたとの報告は地震予知の基礎的条件を満足しなかったため，正しいものでない．この例から地震予知を行う上で多重パラメータ総合システムが重要であることが明らかになった．

2）イタリアはヨーロッパ諸国のなかでは最も地震活動の活発な国の一つであり，現在までにも繰り返し地震被害を受け，耐震設計法の充実を図ってきた国であるが，この地震で大きな被害を受けた．

3）交通系施設としては，交通量の少ない小規模橋梁が落橋したが，全般的には被害を受けるような構造物は少なかったため被害は限定されたものであった．

4）特異な地盤構成を有するラクイラ市と Aterno 川沿いの沖積軟弱地盤上に散在する中小の村落において被害が著しい．ラクイラ旧市街では，地下空洞の崩壊に伴う路面陥没が生じた．

5）ラクイラ市で観測された強震記録により，加速度応答スペクトルは周期0.1～0.5秒で1gを上回る箇所があり，断層近傍の強震動はかなり強いものであった．

6）Aterno 川沿いでは，地盤の滑り，液状化，流動化が，また，周辺の山岳地では落石等が発生した．